Control of electrolysis-generated microbubbles for sensor surface passivation

T. M. Lucas and C. K. Harnett

Citation: Applied Physics Letters **98**, 011915 (2011); doi: 10.1063/1.3541448
View online: http://dx.doi.org/10.1063/1.3541448
View Table of Contents: http://scitation.aip.org/content/aip/journal/apl/98/1?ver=pdfcov
Published by the AIP Publishing

Articles you may be interested in

Frequency dependence and frequency control of microbubble streaming flows
Phys. Fluids **25**, 022002 (2013); 10.1063/1.4790803

Microbubble formation and pinch-off scaling exponent in flow-focusing devices
Phys. Fluids **23**, 092001 (2011); 10.1063/1.3631323

A Novel Solid Electrolyte Oxygen Sensor System for InSitu Measurement and Process Control
AIP Conf. Proc. **1282**, 69 (2010); 10.1063/1.3508561

Underwater microdischarge in arranged microbubbles produced by electrolysis in electrolyte solution using fabric-type electrode
Appl. Phys. Lett. **93**, 231501 (2008); 10.1063/1.3006348

A new device for the generation of microbubbles
Phys. Fluids **16**, 2828 (2004); 10.1063/1.1737739

AIP | Journal of Applied Physics

Journal of Applied Physics is pleased to announce André Anders as its new Editor-in-Chief

This article is copyrighted as indicated in the article. Reuse of AIP content is subject to the terms at: http://scitation.aip.org/termsconditions. Downloaded to IP: 136.165.55.184 On: Tue, 15 Jul 2014 19:34:16

Control of electrolysis-generated microbubbles for sensor surface passivation

T. M. Lucas and C. K. Harnett[a)]
Department of Electrical and Computer Engineering, University of Louisville, Louisville, Kentucky 40208, USA

(Received 5 November 2010; accepted 21 December 2010; published online 7 January 2011)

This letter outlines our work in generating and controlling microbubbles as protective "lids" for samples collected from the environment. The fabrication method uses "strain architecture" to construct three-dimensional cages with high surface area. These structures confine the bubbles and perform as electrodes for electrochemical sample collection and electrolysis-based gas bubble generation. The focus of this article is on the interaction between the microcages and generated bubbles, including the bubble generation mechanism, bubble growth rate, response to hydrostatic pressure, effect of interfacial-tension modifying coatings, and long-term stability. © *2011 American Institute of Physics*. [doi:10.1063/1.3541448]

Gas-trapping microstructures have evolved on plants that develop superhydrophobic surfaces[1] to create a controlled air-water interface. Such structures use geometry at multiple scales to make a tentlike bubble layer as on the fern Salvinia.[2] In microfluidics, bubbles have been used for numerous applications such as particle sorting,[3] inkjet printing,[4] and implementation of Boolean logic.[5] Bubbles can also be detrimental, blocking flow in microchannels[6] and interfering with electrophoretic applications by blocking signals and altering fluid flows.[7] They are unwanted byproducts of electroplating. In all these situations, methods to control and trap microbubbles are of interest.

The devices referenced in this letter consist of a metal electrode that is energized to plate out trace metals from natural water sources. The collected sample is returned to the laboratory for analysis. If left in the field unprotected, a biofilm will form on any electrode surfaces exposed to the water.[8] This film will block reactions between the surface and surrounding solution. A gas bubble could protect the metal surface from water until testing, and then preserve a collected sample from contamination. Such an array of bubble-lidded microcontainers is illustrated in Fig. 1, where a series of metal-lined cages is sequentially exposed to the environment. After releasing a trapped bubble and collecting a sample on the cage walls by electroplating from solution, the bubble is regenerated. The result is a time-stamped archive of the chemical environment.

Stress-mismatched metal-oxide bilayers form three-dimensional (3D) microcages that serve as plating electrodes in the system. Their interaction with bubbles can be modified by changing the surface wettability and cage geometry. The devices are fabricated with a two mask metal and oxide process that has been documented by Moiseeva *et al.*[9]

Figure 2 shows a two-dimensional (a) microcage layout, (b) optical, and (c) electron micrographs of released cages, and arrayed cages within (d) sample wells allowing access to contact pads. The transition from planar to a 3D structure only at the last step means that bubble-generating electrodes can be integrated at the base of the cages in one step [Figs. 2(a) and 2(b)]. This geometry is more difficult to achieve by bulk micromachining, in which features are etched in thick layers of silicon. The result is that bubbles can be electrolytically "inflated" from points inside the cage.

Electrolysis of water occurs at voltages above 1.21 V, which is within the operating range used for electroplating with these devices. However, it is not energetically favorable to form oxygen at until 1.8–2.55 V on metal electrodes.[10] This threshold is an advantage in applying the cages to electrolytic sample collection of trace metals because it reduces bubble formation during routine electroplating.

Heavy metal analysis is commonly performed at low (0.1–1) voltages.[11] These potentials can be applied as long as needed to get a sufficient film on the electrodes. The film growth rate is dependent on factors such as the surrounding metal concentration and the deposition time. The electroplating routine may range from 5 min (Ref. 12) to the order of 1 h (Ref. 13) depending on the application. These low potentials across electrodes are insufficient to create bubbles capable of shielding the surface. This allows for independent bubble growth and electroplating stages of the device operation.

Maximum gas volume (hydrogen plus oxygen) versus time is described in Eq. (1) for 100% efficient electrolysis

$$V_{\text{gas}} = V_{H_2} + V_{O_2} = (3RTIt)/(4FP), \tag{1}$$

where T is temperature, R is the universal gas constant, I is current, t is time, F is the Faraday constant ($F = 96\,485$ C/mol), and P is absolute pressure. However, actual efficiency is reduced by dissolution of oxygen and hydrogen back into solution instead of into the bubble, as well as electrode configuration[14] and Ohmic loss in the aqueous solution.[15] In the bubble trap structure, the efficiency is much below the theoretical maximum.

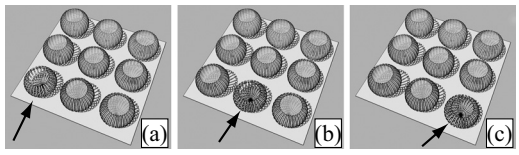

FIG. 1. Array of 300 μm diameter bubble traps undergoing an electroplating sample collection sequence across the front row.

a)Electronic mail: c0harn01@louisville.edu.

 © 2011 American Institute of Physics

This article is copyrighted as indicated in the article. Reuse of AIP content is subject to the terms at: http://scitation.aip.org/termsconditions. Downloaded to IP: 136.165.55.184 On: Tue, 15 Jul 2014 19:34:16

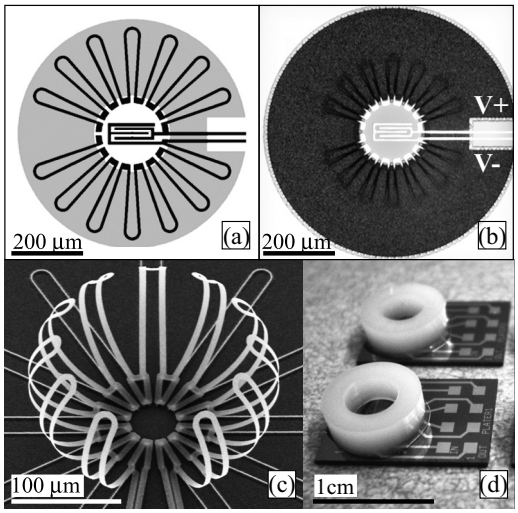

FIG. 2. Released cage devices used for bubble generation and trapping.

Experiments were conducted at voltages ranging from 2.5 to 3 V. The electrodes were set at a constant voltage for 20 min intervals, and the applied current and bubble growth were recorded through LABVIEW software and time-lapse photography at six frames per minute. The images were analyzed for bubble diameter, which was converted to gas volume. By comparing the experimental results with the ideal gas volume equation, the efficiency of the water electrolysis can be determined. Figure 3 compares Eq. (1) with the experimental results and shows images of bubble evolution at different stages during growth; a fit to the results gives 0.8% efficiency for electrolysis-based gas generation.

Bubble volumetric growth is linear with time, and the power input is in the tens of nanowatts. With currents in the 10–20 nA range, and voltages below 3 V, the electrical requirements are well within the resources of a battery-powered autonomous sensor array. At 2.7 V it takes approximately 4 min to fill the microcage. Bubbles nucleate at random points within the cages, which have a metalized inner surface and a hydrophilic oxide outer surface. As they grow, the hydrogen and oxygen bubbles merge and move to the center of the cage. Growth self-terminates if the bubble

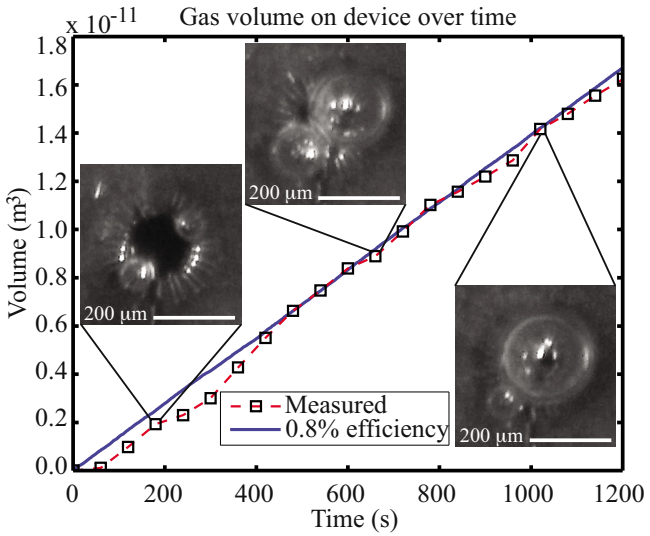

FIG. 3. (Color online) Measured bubble volume present over 20 min plotted beside the ideal gas generation at 0.8%.

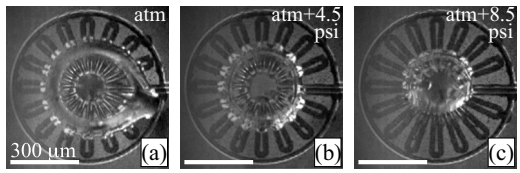

FIG. 4. An air bubble trapped in a microcage in water. The filaments conform to the surface of the bubble over a range of bubble diameters. The outline of the original etch pattern remains on the plane of the substrate, while filaments fold around the bubble.

completely covers the metal and prevents it from further reacting with the water. Octadecanethiol was applied to the device surface in some cases. This self-assembled monolayer rendered the metal hydrophobic and bubbles adhered to the surface longer than on a noncoated device, in agreement with previous work.[16]

Figure 4 is a time series of a bubble confined to a cage as the hydrostatic pressure is increased. Pressure was varied by sealing the sample well, then connecting the chamber through tubing to a regulated nitrogen tank. As the pressure is increased, the filaments conform to the shrinking bubble surface until the force needed to bend them can no longer be supplied by the interfacial tension of the bubble.

The elastocapillary length $L_{EC}=(B/\gamma)^{1/2}$ is the radius of curvature that produces an equilibrium between interfacial energy and strain energy in a filament that contacts an interface.[17] Here B is the bending rigidity $Eh^3/12(1-\nu^2)$, γ is the interfacial tension, E is Young's modulus, h is the filament thickness, and ν is Poisson's ratio for the filament material.

In the structures of Fig. 4, the elastocapillary length of ~ 120 μm is in the same range as the 150 μm cage radius and the overall filament length. Thus the filaments are short enough that they are not immediately destroyed by surface tension, yet are compliant enough to be strongly deflected by the bubble.

The cages have been observed to retain bubbles for a week, in contrast to bare gas bubbles in equilibrium with a solution. Bare bubbles not in contact with a surface are known to have a typical lifetime measured in minutes, with bubbles larger than a critical radius accumulating gas and floating to the surface, and bubbles below the critical radius diffusing gas into solution and dissolving completely. For oxygen in water near saturation, the critical radius is in the range of 100 μm.[18] The cages here (100–300 μm radius) exceed the critical radius and are in the growth regime.

Trapped bubbles must be released to expose fresh plating surfaces. Overinflated bubbles were observed to escape cages having triangular cross-sections by opening the filaments. These interdigitated structures could serve as release valves on the side of a spherical cage.

Microcages with electrodes can stabilize a bubble against both growth and shrinkage, refilling a shrinking bubble by electrolytic gas generation. They can slow the growth of a bubble by forcing a high local curvature (high surface energy) between the filaments where the growing bubble makes contact with the surrounding water. By stabilizing a gas pocket over a surface, these microcages could be useful in underwater chemical sensors that require diffusional contact with dissolved gases. Such structures are also able to reinject gas by electrolysis if the water level rises and

This article is copyrighted as indicated in the article. Reuse of AIP content is subject to the terms at: http://scitation.aip.org/termsconditions. Downloaded to IP: 136.165.55.184 On: Tue, 15 Jul 2014 19:34:16

increases the hydrostatic pressure as shown in Fig. 4.

These advances will improve aquatic sampling platforms in which bubbles are generated through existing electroplating contacts at a higher potential, without additional structures or mechanical parts. Once created, the bubbles are stable at a size large enough to protect a majority of the plating surface—providing surface-passivation options for low-power autonomous sample collection and archiving.

The authors would like to thank Dr. John Naber and Dr. Palaniappan Sethu for their input on the project, and Evgeniya Moiseeva for work with the device fabrication. This work was supported by the National Science Foundation under Grant No. 0644511.

[1]K. Koch, H. F. Bohn, and W. Barthlott, Langmuir **25**, 14116 (2009).
[2]W. Konrad, C. Apeltauer, J. Frauendiener, W. Barthlott, and A. Roth-Nebelsick, J. Bionic Eng. **6**, 350 (2009).
[3]C. C. Chen, J. S. Wang, and O. Solgaard, Sens. Actuators B **117**, 523 (2006).
[4]P.-H. Chen, W.-C. Chen, P.-P. Ding, and S. H. Chang, Int. J. Heat Fluid Flow **19**, 382 (1998).
[5]M. Prakash and N. Gershenfeld, Science **315**, 832 (2007).
[6]J. Kohnle, G. Waibel, R. Cefwosa, M. Stow, H. Ernst, H. Sandmaier, T. Strobelt, and R. Zengerle, Proceedings of the 15th IEEE International Conference on Microelectromechanical Systems, 2002, p. 77.
[7]F. Hallberg, I. Furo, P. V. Yushmanov, and P. Stilbs, J. Magn. Reson. **192**, 69 (2008).
[8]D. Yan, Z.. Bai, M. Rowan, L. Gu, R. Shumei, and P. Yang, J. Environ. Sci. (China) **21**, 834 (2009).
[9]E. Moiseeva, Y. M. Senousy, S. McNamara, and C. K. Harnett, J. Micromech. Microeng. **17**, N63 (2007).
[10]J. Rossmeisl, A. Logadottir, and J. K. Nørskov, Chem. Phys. **319**, 178 (2005).
[11]P. R. M. Silva, M. A. El Khakani, M. Chaker, G. Y. Champagne, J. Chevalet, L. Gastonguay, R. Lacasse, and M. Ladouceur, Anal. Chim. Acta **385**, 249 (1999).
[12]X. Xie, D. Stüben, Z. Berner, J. Albers, R. Hintsche, and E. Jantzen, Sens. Actuators B **97**, 168 (2004).
[13]C. K. Harnett, E. V. Moiseeva, B. Casper, and L. Wilson, Proceedings of the IEEE International Instrumentation and Measurement Technology Conference, Austin, TX, 2008, p. 328.
[14]K. Onda, T. Kyakuno, K. Hattori, and K. Ito, J. Power Sources **132**, 64 (2004).
[15]N. Nagai, M. Takeuchi, and M. Nakao, JSME Int. J., Ser. B **46**, 549 (2003).
[16]J. Yang, J. Duan, D. Fornasiero, and J. Ralston, J. Phys. Chem. B **107**, 6139 (2003).
[17]C. Py, P. Reverdy, L. Doppler, J. Bico, B. Roman, and C. N. Baroud, Phys. Rev. Lett. **98**, 156103 (2007).
[18]A. S. Tucker and C. A. Ward, J. Appl. Phys. **46**, 4801 (1975).

This article is copyrighted as indicated in the article. Reuse of AIP content is subject to the terms at: http://scitation.aip.org/termsconditions. Downloaded to IP: 136.165.55.184 On: Tue, 15 Jul 2014 19:34:16